# Regression rate study in a small Hybrid Rocket Engine using $N_2O$/Paraffin propellants

*Karim Boughaba* and Patrick Hendrick**
**Université Libre de Bruxelles*
*F.D. Roosevelt Avenue 50, 1050 Brussels, Belgium*

## Abstract
Hybrid rocket engines are promising to replace solid and liquid rockets due to their inherent safety, throttling capability and environmentally green exhaust gases. The main disadvantage is the low regression rate and thus the low Isp. Université Libre de Bruxelles has developed a test bench in order to characterize the paraffin/nitrous oxide couple of propellants in a first step and improve the regression rate through the injection optimization and the addition of metallic additives in a second step. Results are quite interesting with mean regression rate of ~5mm/s for pure paraffin wax.

## Nomenclature

| | |
|---|---|
| AP | Aluminium perchlorate |
| Gox | oxidizer mass flux [kg/( $m^2$s)] |
| Gox | gazeous oxygen |
| HRE | hybrid rocket engine |
| HTPB | Hydroxyl-Terminated PolyButadiene |
| Isp | Specific impulse [s] |
| $\dot{m}_{ox}$ | oxidiser mass flow [kg/s] |
| $N_2O$ | nitrous oxide |
| O/F | oxidiser to fuel ratio |
| P-T | pressure-temperature |
| $\dot{r}$ | regression rate [mm/s] |
| SV | Solenoid valve |

## 1. Introduction

Since the end of 2006, ULB is developing a test bench to study the Paraffin/$N_2O$ regression rate. Throughout the tests, 3 engines were constructed with some improvements at each step to ensure proper data acquisition and safe firing. The purpose is to obtain a representative 1kN thrust engine and measure the regression rate.
After a presentation of the test bench, we will broach on cold test that enable us to characterize the nitrous oxide flow. This leads to several modifications on the line in order to increase the mass flow and to reduce head losses.
Finally we will present the hot test campaign that is divided into 3 parts, where regression rate is analysed for different configurations of paraffin grain.

## 2. Test bench description

The test bench is composed of five parts: the injection line, the ignition part, the combustion chamber, the nozzle and the venting.

The injection line (Fig. 1) is composed of three $N_2O$ bottles in parallel. Each one is equipped with a 1/4" hose and a solenoid valve to control independently each one. The three bottles merge on a 1/2" hose, which is connected to the engine through an injector. The solenoid valve was the main concern during the first versions of the engine. In fact, the $N_2O$ vaporization drops the temperature well below 0°C, that causes the previous versions of the solenoid valve to freeze and conducts to a malfunction which prevents us from starting the injection. The ¾” solenoid valve in the

first engine version is replaced by three ¼" valves dedicated to NOS system used in competition cars and studied for $N_2O$ flow.

Figure 1: $N_2O$ Injection line

For the tests, two types of injectors (Fig. 2) were used: a hollow cone and a full cone pattern injector. The first one has an angle spray of 50° and the second one of 60°.

Figure 2: Full cone (left) and hollow cone (right) injectors

Measuring the flow is very difficult, even with a Coriolis flow meter because it is a two-phase flow. To deal with this issue, the bottles are mounted on a strain gauge and as in our case the flow is constant (Fig. 3), it is given by the slope.

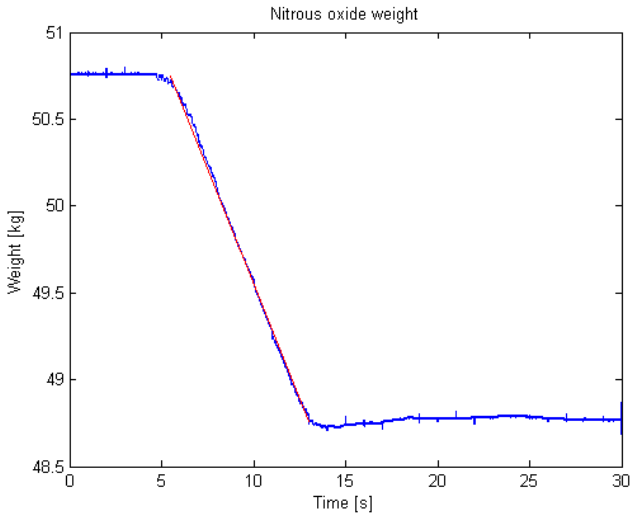


Figure 3 : $N_2O$ weight versus time

A pyrotechnic cartridge made in collaboration with the Royal Military Academy of Belgium commands the ignition. It is composed of four elements (from left to right in Fig. 4):
- a professional igniter
- spherical powder
- ignition powder
- extruded grain made from AP/Kraton/Aluminum.

The mixed grain is extruded and after several tests, we obtain the following dimensions for optimal engine start:
- 45 mm length
- 21.5 mm outside diameter
- 8 mm inside diameter

Prior to any combustion test, the effect of the pyrotechnic cartridge only on the paraffin grain is observed. The results demonstrate that the paraffin grain loses a few grams of material and is not affected by this one. Thus the influence must not be taken into account when the regression rate is calculated.
The temperature attains a value exceeding 1200°C which is highly above the $N_2O$ dissociation temperature and ensures the start of the combustion.

Figure 4: Pyrotechnic components

The engine is made of steel and is composed of three parts:
- the precombustion chamber
- the combustion chamber & the afterburner
- the nozzle.

The precombustion chamber (Fig. 5) permits the $N_2O$ vaporization and dissociation before reacting with the melting paraffin inside the combustion chamber. It is equipped with three type K thermocouples equally distributed along the circumference and a housing for the ignition cartridge. The central port is the injection line entry. A pressure sensor is used in the precombustion chamber to ensure a minimum of 20% pressure drop between this one and the injection line. It is the minimum recommended value given in [1] to prevent hot exhaust gas flowback.

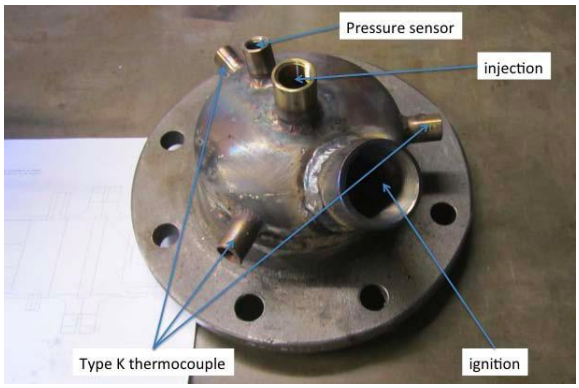


Figure 5: Precombustion chamber

The combustion chamber (Fig. 6) is the central part of the engine. It is longer than the grain and the empty space serves as an afterburner to let the propellant react and have better combustion efficiency. In order to avoid the paraffin grain embedding into the injector and a reaction in the outer face, a ring is placed between the precombustion and the combustion chamber. Two sensors capture the pressure and the temperature, using a type C thermocouple.

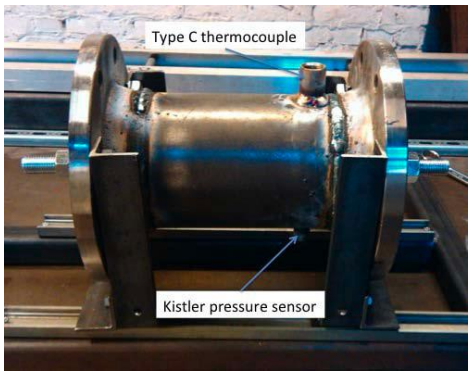


Figure 6: HRE combustion chamber

The nozzle (Fig. 7 right) closes the engine. It is made of graphite, which resists better to abrasion and is fitted in a piece (Fig. 7 left) that gives a smooth transition to the gases before the exit. It is a simple convergent-divergent nozzle with a 22mm throat diameter and a 44.9 mm exit diameter having thus an expansion ratio of 4.17.

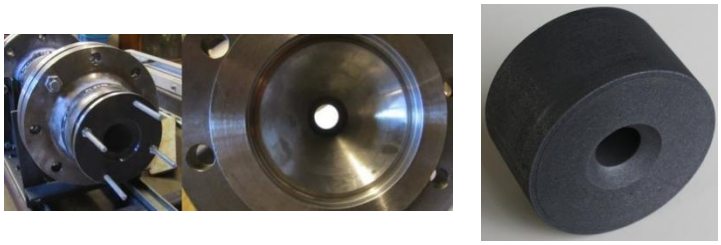

Figure 7: Graphite Con-Di nozzle and its support

To prevent the hot exhaust gas from entering the line after the combustion test and avoid a $N_2O$ dissociation reaction [2], it was decided to add a venting line using $N_2$ at 10 bar to eject the residual hot gazes inside the combustion chamber and prevent any explosion hazard.

## 3. Experiments

### 3.1. Injection tests

Prior to any combustion, multiples cold tests were done in order to characterize the injection line. Our goal is to reach a 1 kN thrust engine.
Difficulties encountered in the nitrous oxide injection system development were confirmed by several sources citing this part of a nitrous oxide fed hybrid rocket as a neuralgic point. Nitrous oxide's advantage of being self-pressurized at ambient temperature brings with it the problem of its very high sensitivity to oxidizer feed line pressure losses causing rapid vaporization and hence a largely reduced available mass flow rate at the entrance of the combustor. In order to size our test bench correctly for future tests, an analysis of the phenomenon and of solutions available to cope with this pressure loss problem has been undertaken.
The first idea was to use a manual gate valve to control the flow and the thrust by the way. The first test gives the results shown in Figure 8.

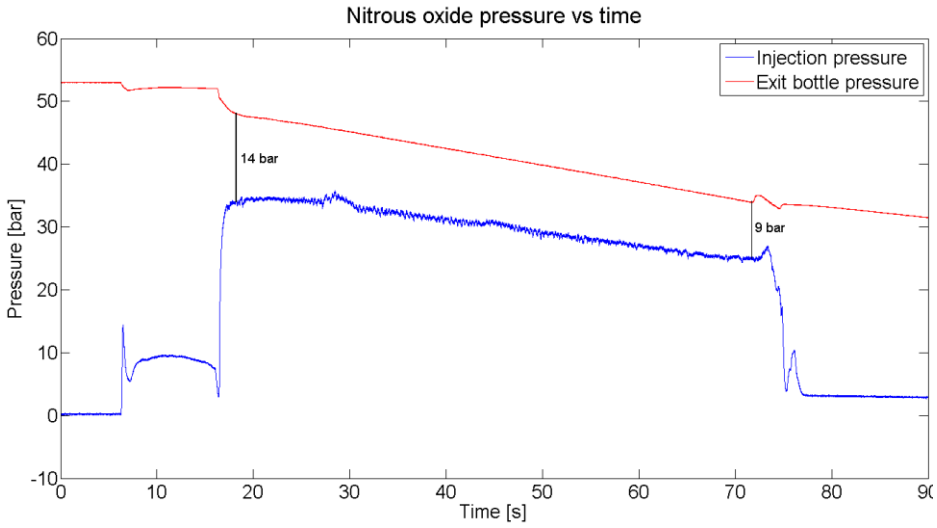


Figure 8: Pressure evolution during the 1st injection test

We observe high head losses in the line. The P-T diagram (Fig. 9) clearly indicates that the vapour phase is dominant in the flow.

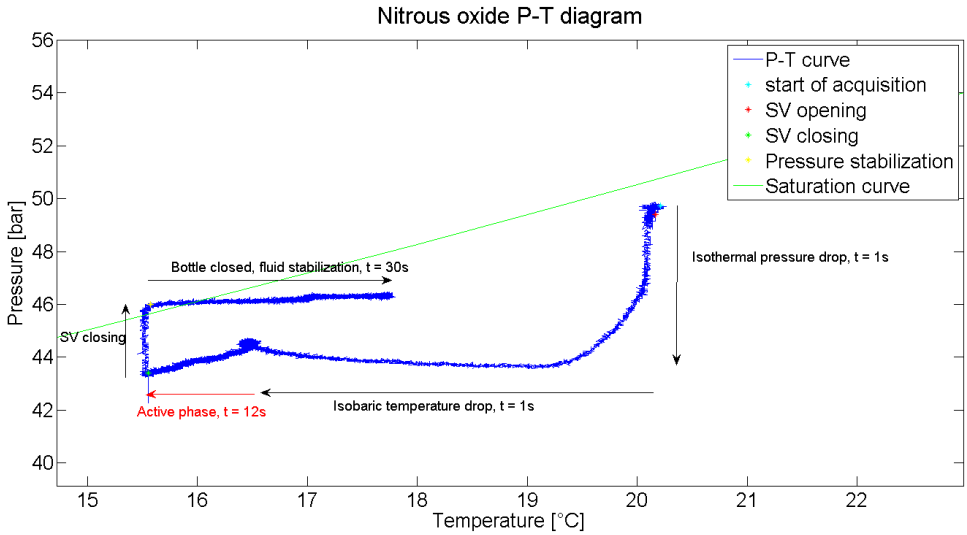


Figure 9: P-T diagram during the 1st injection test

The second phase of the study consists of the head losses measurement of each injection line component. We found from the study that the manual gate valve is responsible of a 10 bar pressure drop. So it was decided to remove it. Figure 10 gives the flow in a P-T diagram without manual gate valve.

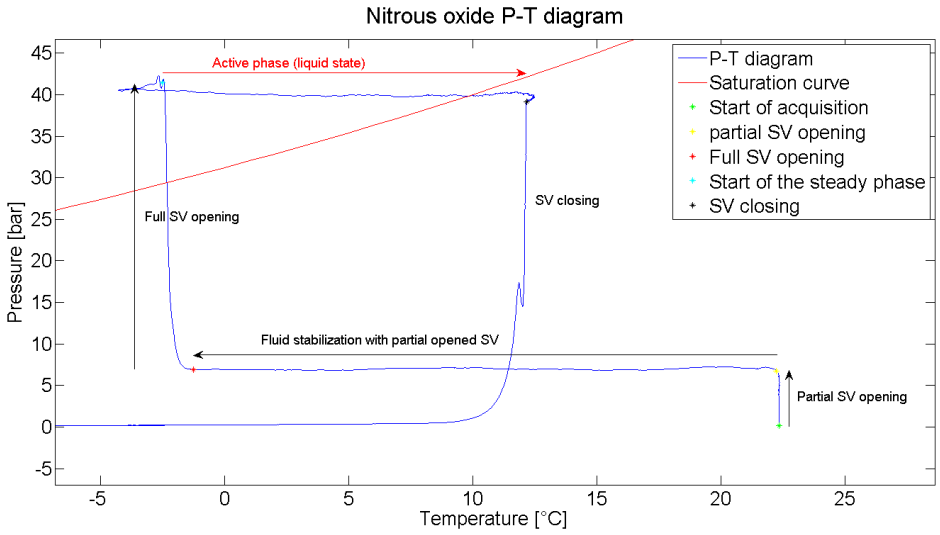


Figure 10: P-T diagram for the 2nd test

The curve shifts upwards, above the saturation line, indicating a liquid phase in the injector. This ensures proper atomization of the $N_2O$ and a better combustion inside the chamber.
Despite the increase of performance, the flow is too low to reach a 1 kN thrust. As gas companies deliver the bottles, they are studied for medical application and the exit orifice induces important head losses. The goal is to vaporize the $N_2O$ to put to sleep the patient.
To increase it, three solutions were envisaged:
- the use of the NOS system for competition cars with a pressurization system,
- the construction of an intermediate tank,
- the use of multiple bottles in parallel.

The first solution is elegant as the system comprises a pressurization entry but once the bottles are empty, it is not possible to fill them by gas suppliers. Moreover, the flow is too low for our application.
The second solution is difficult because the tank must be tested until burst and it raises security problems and a lack of infrastructures.
So the easier and safest way is to put multiple bottles in parallel. Even with 3 bottles, the flow is lower than expected. So the only solution will be to construct an intermediate tank with a larger exit orifice and a pipe with 2 entries: one for pressurization and one as exit. It will solve the vaporization problem and ensure a fluid phase all along the line.

## 3.2. First hot tests campaign

17 tests were made in order to characterize the $N_2O$/paraffin regression rate. All of them are launched using a LabView interface that controls the timing.
The sequence starts with the ignition, followed by the injection. After a pre-defined combustion duration, the oxidant flow is stopped and $N_2$ is injected in the engine for venting to prevent any explosion hazard. The remaining paraffin is weighted to know how much fuel has reacted.

The time-averaged regression rate is given on Figure 11. As we can observe, the mean regression rate is around 4 to 5 mm/s. As read in existing literature, it is higher than for HTPB/$N_2O$ (1 mm/s) [3] as expected but more surprisingly, the value is also higher than the values found in literature for the same fuel/oxidant (3 mm/s) [4]. In fact, we found results very equivalent to the results with SP-1a paraffin/GOX used by the University of Stanford [5].

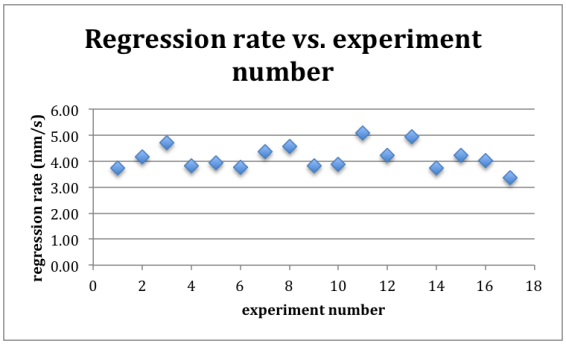


Figure 11: Regression rate

In Figure 12, we have the mean O/F ratio given for each experiment. We observe that the values are below the design value of 6.7, which gives the best theoretical $I_{sp}$.

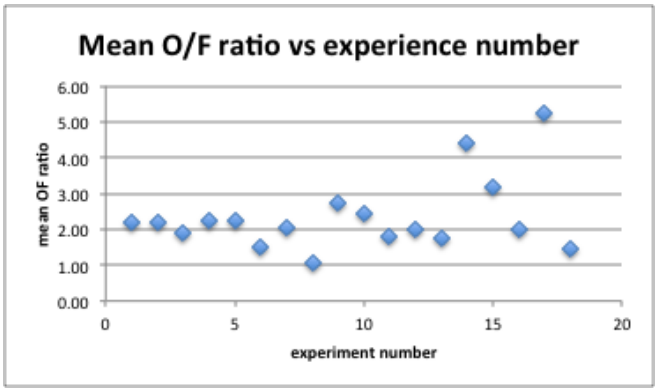


Figure 12: Mean O/F ratio

This is coherent with the tests video where a lot of smoke is observed in the exhaust flame, indicating that the paraffin has not fully reacted during combustion. This fact explains why the calculated $I_{sp}$ (Fig. 13) is far below the theoretical values.

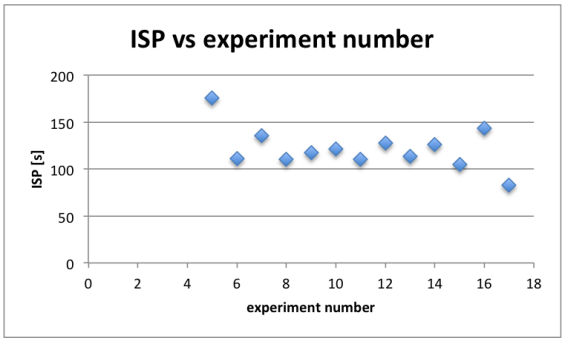


Figure 13: Obtained ISP

The results can be explained due to a bad vaporization of the $N_2O$ flow that ejects the paraffin without reacting or by an incomplete combustion due to a too short stay in the afterburner. Further tests will permit to determine the cause.

### 3.3. Varying length combustion tests

When observing the previous tests, we observe that a lot of smoke composed of unburned paraffin is ejected through the nozzle. It has as consequences a loss of energy and the specific impulse is low compared to the theoretical curve. As the design oxidizer flow cannot be reached due to injection line limitations and in order to increase the O/F ratio, it was decided to shorten the paraffin grain length and study its influence on the engine performance.
Four tests were conducted with a paraffin grain length of 19, 15, 10 and 5 cm. The results are given in Table 1.

Table 1: *Results comparison for varying paraffin grain length*

| Grain length (cm) | Injection time (s) | $\dot{r}$ (mm/s) | Isp (s) | Gox (kg/(m².s)) | $\dot{m}_{ox}$ (kg/s) | O/F | Mean thrust (N) | Total mass flow (kg/s) |
|---|---|---|---|---|---|---|---|---|
| 19 | 9.11 | 5.38 | 91.73 | 41.66 | 0.189 | 0.96 | 357.9 | 0.39 |
| 15 | 7.316 | 6.70 | 95.8 | 77.37 | 0.351 | 1.76 | 593.91 | 0.55 |
| 10 | 5.65 | 8.67 | 94.25 | 72.96 | 0.331 | 2.02 | 549.86 | 0.5 |
| 05 | 6.8 | 7.21 | 151.41 | 64.15 | 0.291 | 4.4 | 517.04 | 0.36 |

The first observation is the increase of the regression rate with the decrease of paraffin length except for the 5 cm length. The lower regression rate is due to a lower oxidizer flow for this test.
The engine performance is also increased as the paraffin length is reduced. If we observe the specific impulse, it is almost constant at 90s for the 19, 15 and 10 cm length followed by an increase for the 5 cm paraffin grain length. The result is that we have the same amount of thrust for the 5 cm configuration even if the total flow is reduced to 0.36 kg/s compared to the 0.5 kg/s for the previous test.
As expected, the O/F ratio is increasing with the decreasing length with a reached O/F of 4.4 for the 5 cm grain length. It is still below the 6.7 design value but this value is a mean value over the entire test.
By observing the screenshots from the tests videos (Fig. 14 to 17), we can observe the change in the exhaust flame with decreasing paraffin length. When the length is 19 and 15 cm, the exhaust flame contains a high proportion of unburned paraffin that exits the engine without providing its energy. As the paraffin length is reduced, the performance starts to be better. For the 10 cm length, the exhaust flame is wide indicating that there is a proportion of unburned paraffin reacting with the surrounding air. For the 5 cm length, the exhaust flame is straight indicating a good combustion. There is no reaction zone around the flame. This is confirmed using the K-type thermocouple. In the first 3 tests, the combustion temperature is slightly below 1200°C but for the 5 cm grain length, the thermocouple is destroyed indicating a temperature well beyond 1200°C.

*Figure 14: A 19 cm combustion test*

*Figure 15 : A 15 cm combustion test*

*Figure 16 : A 10 cm combustion test*

*Figure 17 : A 5 cm combustion test*

As the 5 cm grain length is delivering the best performance, the new engine is to be designed to study the regression rate with this paraffin grain length.

### 3.4. Tests with a 5 cm grain length

#### 3.4.1. Tests results

As seen previously the 5 cm grain length gives the best performance. So a new engine was designed following the rules given in [1]. The combustion chamber has a length of 17.5 cm compared to the 29.7 cm of the first version. Figure 18 gives a picture of the two HRE combustion chambers.

*Figure 18 : Engine combustion chamber for the two design lengths*

Some changes were added to this new engine: the inner port radius is reduced to 2.7 cm to increase the initial oxidizer flux, a ring is added between the precombustion and the combustion chamber to avoid a forward move of the grain and a combustion taking place on the outer side and finally the grain is moulded directly inside the engine to avoid combustion on the outer part.
The test campaign comprises 9 tests: the first one is described here above and it is a validation test then 6 tests were done with an injection time ranging from 1 to 8 s. The purpose is to retrieve the ‘a’ and ‘n’ coefficient from the regression law. Finally two others tests of 2 s were done in order to confirm the high regression rate found.
Table 2 gives the results found for the 9 tests. They are sorted by increasing injection time.

Table 2 : 5 cm grain length combustion tests results

| Test | 2 | 9 | 8 | 3 | 4 | 5 | 6 | 1 | 7 |
|---|---|---|---|---|---|---|---|---|---|
| Injection time (s) | 1.217 | 2.025 | 2.277 | 2.333 | 3.369 | 4.356 | 6.415 | 6.8 | 7.851 |
| $\dot{r}$ (mm/s) | 14.60 | 11.25 | 9.88 | 8.15 | 10.57 | 5.90 | 6.94 | 7.21 | 7.32 |
| Isp (s) | 68.88 | 121.10 | 154.98 | 173.86 | 153.28 | 173.03 | 171.69 | 151.41 | 155.99 |
| Gox (kg/(m².s)) | 116.23 | 96.60 | 125.21 | 138.87 | 99.11 | 139.47 | 67.47 | 64.15 | 47.29 |
| $\dot{m}_{ox}$ (kg/s) | 0.183 | 0.188 | 0.241 | 0.231 | 0.305 | 0.304 | 0.271 | 0.291 | 0.265 |
| O/F | 2.23 | 2.67 | 3.92 | 4.90 | 3.67 | 7.79 | 4.35 | 4.40 | 3.41 |
| Mean thrust (N) | 262.73 | 364.98 | 436.07 | 479.69 | 519.72 | 463.16 | 528.02 | 517.04 | 510.87 |
| Total mass flow (kg/s) | 0.27 | 0.26 | 0.30 | 0.28 | 0.39 | 0.34 | 0.33 | 0.36 | 0.34 |

The first observation (Fig. 19) is that the O/F ratio is increased to a maximum value of 7.79 for the 5 cm grain length and the specific impulse is better than with the 19 cm grain length. It is now around 160 s. The engine still needs to be improved to increase this value. Injector, post combustion length and the nozzle must be optimized in order to increase the specific impulse. As shown in Figure 20, the exhaust flame is convergent at the nozzle exit indicating an overexpanded flow. This is because the nozzle is designed for an oxidizer mass flow of 0.45 kg/s and a combustion chamber of 25 bar where we have a mass flow of maximum 0.3 kg/s and a pressure around 12 bar.

Figure 21 shows the calculated oxidizer flux versus the mass flow. As expected, the flux is increased as the inner port radius is reduced. The effect is that the regression rate is much higher than the first design.

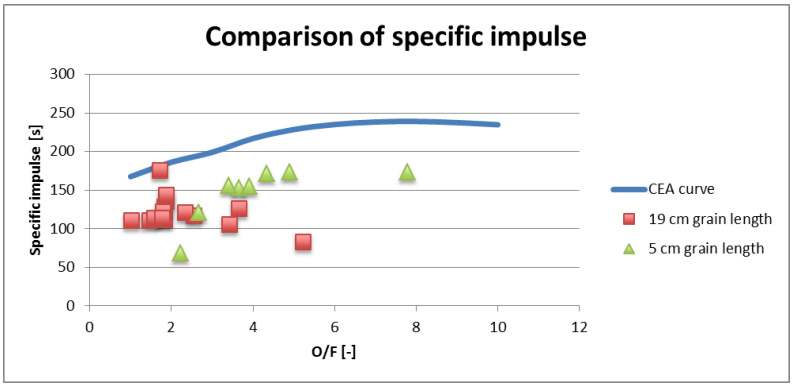


Figure 19 : Specific impulse for theoretical case, 19 cm and 5 cm grain lengths

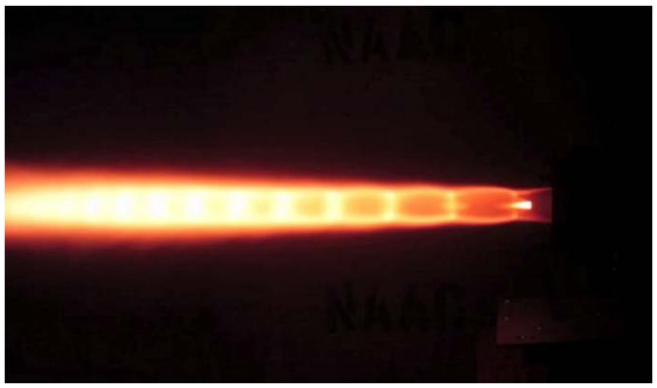

Figure 20 : Exhaust flame of a 5 cm grain length

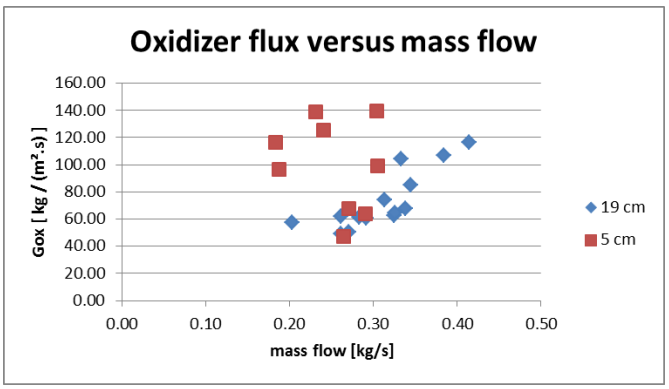


Figure 21 : Gox vs. oxidizer mass flow

### 3.4.2. Regression rate study

Using the same methodology as [3], a regression rate study is achieved based on the new engine design. The methodology to weight the grain for tests 8 and 9 differs from the others. For test 1 to 7, the combustion chamber containing the grain is weighted before and after the combustion test. The difference gives the portion of paraffin that reacts during the given combustion time. For the two last tests, the paraffin is weighted using a precision weighting scale before the test. At the end of the test, the remaining paraffin is extracted from the engine and is weighted again. The difference gives the weight of paraffin that has reacted. When comparing test 3 with tests 8 and 9, we found respectively 110, 140 and 142.5 g. This indicates that the first method underestimates the reacting weight of paraffin and thus the regression rate.

In order to assess the results, $\dot{r}$ calculated using the same method as [3] is compared to $\dot{r}_m$ calculated using eq. 1. The inner port radius is measured for each grain at the end of the combustion and this gives us the regression rate $\dot{r}_m$ where $R_f$ and $R_i$ are the final and initial port radius in meter and $t_b$ is the burning time in s.

$$\dot{r}_m = \frac{(R_f - R_i)}{t_b} \quad (1)$$

In Table 3, $R_{f,c}$ is the final radius calculated using eq. 2.

$$R_{f,c} = R_i / 2 + \dot{r} * t_b \quad (2)$$

$R_{f,m}$ is the measured radius at the end of each test.

$m_{fuel}$ is the measured weight of paraffin that has reacted and $m_{fuel,c}$ is the weight of paraffin corresponding to the measured final radius. It is given by eq. 3.

$$m_{fuel,c} = \pi * (R_f^2 - R_i^2) * l_g * \rho_f \quad (3)$$

Table 3 gives the results for the test campaign. The initial port radius is 2.7 cm.

Table 3 : Regression rate for the 5 cm grain length

| Test | 2 | 3 | 4 | 5 | 6 | 7 |
|---|---|---|---|---|---|---|
| Injection time (s) | 1.217 | 2.333 | 3.369 | 4.356 | 6.415 | 7.851 |
| $\dot{r}$ (mm/s) | 14.60 | 8.15 | 10.57 | 5.90 | 6.94 | 7.32 |
| $\dot{r}_m$ (mm/s) | 3.70 | 4.71 | 5.94 | 5.05 | 5.85 | 6.56 |
| Difference (%) | 394.96 | 172.92 | 177.98 | 116.73 | 118.70 | 111.59 |
| $R_{f,c}$ (mm) | 31.27 | 32.52 | 49.10 | 39.18 | 58.01 | 70.97 |
| $R_{f,m}$ (mm) | 18 | 24.5 | 33.5 | 35.5 | 51 | 65 |
| Difference (%) | 173.74 | 132.74 | 146.56 | 110.37 | 113.75 | 109.18 |
| $m_{fuel}$ (g) | 100 | 110 | 280 | 170 | 400 | 610 |
| $m_{fuel,c}$ (g) | 17.81 | 52.53 | 118.12 | 135.47 | 303.95 | 508.03 |
| Difference (%) | 561.39 | 209.41 | 237.04 | 125.49 | 131.60 | 120.07 |

The first observation is the very high regression rate found for the 1s test when compared to the one found geometrically. The measured inner radius corresponds to a mass of fuel of 17.81 g. As it is not possible to consume so less fuel, the explanation of the discrepancy between the two values is due to the fact that the paraffin grain burns in the front face wheras the measured radius do not take into account this part of burned paraffin. So the fuel mass used to calculate the regression rate do not consider only the regression on the inner radius but on all the faces. As the burning time is increased, the discrepancy becomes lower to reach a value of 10% difference for the 8 s injection time test.

The value of the regression rate is higher by 140% compared to the previous test (~5 mm/s). This is coherent with the experiments as the grain burns completely in 8 s for the 5 cm grain length compared to 12 s for the previous design so a ratio of 150% that is in the same order.
This increase can be explained by a much better combustion as the O/F ratio is shifted towards the higher value. As consequence the combustion temperature is higher and so the heat flux to the paraffin that impacts the melting and the regression rate.
Compared to literature ([6][5]) that shows a regression rate of respectively 2 mm/s and 3.5 mm/s, we have an increase of respectively 350 and 200%. Compared to the first results, this can be explained by the following factors:

- The cylindrical geometry offers more area so the heat flux is more important
- The use of nitrous oxide compared to Gox increases the regression rate as it is proportional to the dynamic pressure following the work from Karabeyoglu.

As of today we cannot explain the great discrepancy between our results and the one found in [5].

## 4. Conclusions and perspectives

The hot tests give encouraging results and the $N_2O$/paraffin couple gives a higher regression rate than $N_2O$/HTPB. That implies that the $N_2O$/paraffin engine could be more compact.
The injection line can be improved by the construction of a pressurized tank that permits to increase the flow and to have a fluid phase in the injectors.
The ignition cartridge is very reliable, as we do not notice any malfunction during all the tests.
In order to retrieve the ‘a’ and ‘n’ coefficient of the regression law, a device is developed to measure in real time the thickness of the paraffin grain. It is composed of a printed circuit board with electrical resistances in parallel and molded in the grain. When the grain is burning, the resistances are destroyed and we can observe a voltage step in the LabView interface. The circuits are shown in Figure 22.

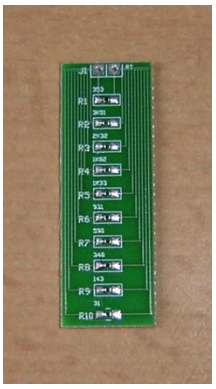

Figure 22: Regression rate sensor

Once the sensor is ready to be used, further work is planned with some additives in the paraffin grain such as metallized particles with the objective to study the effect on the regression rate.

## Acknowledgements

The authors of this study would like to express their thanks and acknowledgments to ESA-ESTEC for their support and financial assistance in this project. This work was performed within the "Future High Altitude High Speed transport 20XX" (FAST20XX) FP7 project investigating high speed transport concepts. The project is coordinated by ESA-ESTEC and supported by the European Union within the 7th Framework program theme 7 transport, Contract no: ACP8-GA-2009-233816. Further information on FAST20XX can be found on http://www.esa.int/fast20xx.

## References

[1] Colburn, W. H. 2005. A Manual for Hybrid Propulsion System Design. Edited by Steven Zwaska.
[2] Thicksten, Z., F. Macklin and J. Campbell. 2008. Handling Considerations of Nitrous Oxide in Hybrid Rocket Motor Testing. In: 44th AIAA/ASME/SAE/ASEE Joint Propulsion Conference & Exhibit, Hartford, CT, 21 - 23 July 2008.
[3] Doran, E., J. Dyer, Z. Dunn, K. Lohner and G. Zilliac. 2006. Fuel regression rate characterization using a laboratory scale nitrous oxide hybrid propulsion system. In: 42nd AIAA/ASME/SAE/ASEE Joint Propulsion Conference & Exhibit, Sacramento, California, USA.
[4] Azimi, S., M. Hultgren, A. McCormick, J. Smith and R. Sneed. 2005. Design, optimization and launch of a 3inch diameter N2O/Aluminized paraffin rocket. In: 41st AIAA/ASME/SAE/ASEE Joint Propulsion Conference, Tuscon, Arizona, USA.
[5] Dyer, J., K. Lohner, E. Doran, Z. Dunn, Z., A. Sadhwani, A. Chemistruck, C. Bayart, P. Nesline, C. Cheung, G. Zilliac, A. Karabayaglu, and B. Cantwell. Design and development of a 100km nitrous oxide/paraffin hybrid rocket engine. 2006. In: 43nd AIAA/ASME/SAE/ASEE Joint Propulsion Conference & Exhibit, Cincinati, Ohio, USA.
[6] MEROTTO, L., M. Boiocchi, A. MAZZETTI, F. MAGGI, L. GALFETTI, and L.T. DE LUCA. 2011. Characterization of a family of paraffin-based solid fuels. In: 4TH European conference for aerospace sciences, Saint Petersburg.